Synthesis, Crystal Structure and Biological Activity of 2-[(Pyridin-2-yl)methylthio]-1*H*-benzimidazole Derivatives

GAO Di(高迪)[1,2];CHEN Gu-Zhou(陈固洲)[2];CAO Sheng(曹胜) [2];DU Yue(杜月) [2];JIN Zhe(金辄)[2];LIU Xiao-Ping(刘晓平)[2];OUYANG Gui-Ping(欧阳贵平) [1];HU Chun(胡春) [1,2]

[1] *Key Laboratory of Green Pesticide and Agricultural Bioengineering, Ministry of Education, Research and Development Center of Fine Chemicals, Guizhou University, Guiyang* 550025, *China*;[2] (*Key Laboratory of Structure-based Drug Design & Discovery, Ministry of Education; Shenyang Pharmaceutical University, Shenyang* 110016, *China*

ABSTRACT In order to discover the novel anti-tumor agents, a series of 2-[(pyridin-2-yl)methylthio]-1*H*-benzimidazole derivatives were designed and synthesized, and the structures were characterized by IR, MS, and proton NMR. 2-[(3,4-Dimethoxypyridin-2-yl)methylthio]-1H-benzimidazole was investigated with X-ray crystallography, and the molecule is in orthorhombic system, space group $P2_12_12_1$, with a = 9.1828(16), b = 11.625(2), c = 13.463(2) Å, Z = 4, R = 0.0231 and wR = 0.0596. The antitumor activities of target compounds were evaluated against human liver cancer cell line HepG2, and human liver normal cell line HL7702 using MTT assay. The target compounds have demonstrated weak or moderate anti-tumor activity against HepG2, while all the target compounds exhibit no cytotoxic effects on HL7702.

Keywords: 2-[(pyridin-2-yl)methylthio]-1*H*-benzimidazole derivatives; synthesis; crystal structure; antitumor activity; DOI: 10.14102/j.cnki.0254-5861.2011-1730

1 INTRODUCTION

Nowadays a large number of populations were affected by cancers all around the world. Only in 2012, 14.2 million new cancer cases and 8.2 million deaths had happened unfortunately, and up to 2030 it is reported to increase to about 19 million[1].

In recent decades, the benzimidazole derivatives were discovered to exhibit various biological activities such as antibacterial, antiviral, antiallergic, cardiovascular, antitumor, analgesic, antiiflammatory, H^+/K^+-ATPase inhibitory and antipyretic activities[2]. The benzimidazole derivatives with pyridyl group have reported to demonstrate potent anticancer and antitumor activities. For example, the benzimidazole derivatives with 2-pyridylethyl moiety at the 2-position displayed inhibitory effects on the proliferation of murine leukemia cells (L1210/0) and human T-lymphocyte cells (Molt 4/C8 and CEM/0) with the IC_{50} values in the low microgram range[3, 4]. Some 2-[3-(pyridin-3-yl)styryl]-1*H*-benzimidazole derivatives have exhibited antiproliferative activity against HeLa, HepG2, A498, MCF-7 and U937 cell lines[5]. The hybrid compounds with benzimidazole ring and pyridine skeleton were designed and evaluated against NCI 60 cell lines, and the screening results show some compounds exhibit a very good antitumor activity against renal cancer A498 and breast cancer MDA-MB-468 and also present a significant antitumor activity against leukemia (RPMI-8226, CCRF-CEM, K-562, SR), non-small cell lung cancer (NCI-H23, A549/ATCC), and breast cancer T-47D[6].

According to the antitumor structure-activity relationship of benzimidazole derivatives, principle of bioisosterism and hybridization, a series of 2-[(pyridin-2-yl)methylthio]-1*H*-benzimidazole derivatives were designed and synthesized as the target compounds. The synthesis of the target compounds is shown in Scheme 1, according to the reported procedure[7-11].

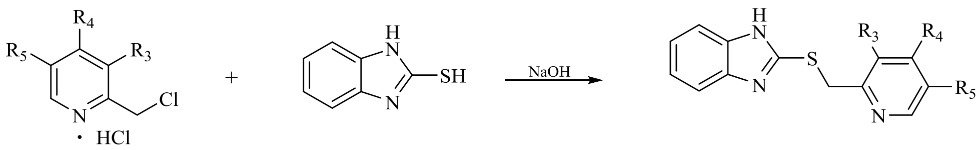

1 2 3

1a: $R_3 = R_5 = CH_3$, $R_4 = OCH_3$
1b: $R_3 = R_5 = OCH_3$, $R_5 = H$
1c: $R_3 = OCH_3$, $R_4 = OCH_2CF_3$, $R_5 = H$
1d: $R_3 = CH_3$, $R_4 = O(CH_2)_3OCH_3$, $R_5 = H$

3a: $R_3 = R_5 = CH_3$, $R_4 = OCH_3$
3b: $R_3 = R_5 = OCH_3$, $R_5 = H$
3c: $R_3 = OCH_3$, $R_4 = OCH_2CF_3$, $R_5 = H$
3d: $R_3 = CH_3$, $R_4 = O(CH_2)_3OCH_3$, $R_5 = H$

Scheme 1. Synthesis of the target compounds

The target compounds were characterized by IR, proton NMR, and ESI-MS. Fortunately, a single crystal of a target compound was grown, and the structure was characterized by X-ray diffraction analysis. The preliminary pharmacological test showed all target compounds exhibit weak or moderate cytotoxicity against human liver cancer cell line HepG2 and no cytotoxic effects on the human liver normal cell line HL7702.

2 EXPERIMENTAL

2. 1 Apparatus and materials

The melting points were determined on a melting-point apparatus with microscope (Zhengzhou Mingyi Instrument Equipment Co., Ltd., Zhengzhou, China), and were uncorrected. ESI mass spectra were performed on a Waters spectrometer (Waters Corporation, USA). The IR spectra were recorded on a Bruker IFS55 spectrometer (KBr pellets). ^{1}H NMR spectra were recorded on a Bruker (400 MHz) NMR spectrometer (Faellanden, Switzerland) with TMS as an internal standard and $CDCl_3$ as the solvent. Chemical shifts (δ values) and coupling constants (J values) are respectively given in ppm and Hz.

All the starting materials were commercially available and directly used without further purification. All the reaction progress was monitored by thin layer chromatography analysis with the silica gel plates (Qingdao Jiyida silica reagent factory, Qingdao, China).

2-Chloromethyl-4-methoxy-3,5-dimethylpyridine hydrochloride, 2-chloromethyl-3,4-dimethoxypyridine hydrochloride, 2-chloromethyl-3-methyl-4-(2,2,2-trifluoroethoxyl)pyridine hydrochloride, and 2-chloromethyl-4-(3-methoxypropoxy)-3-methylpyridine hydrochloride were prepared by previously reported procedures[7, 8].

2. 2 Synthesis and characterization

A mixture of 2-chloromethyl-4-methoxy-3,5-dimethylpyridine hydrochloride (0.0040 mol), 1*H*-benzimidazole-2-thiol (0.0040 mol), 40% sodium hydroxide aqueous solution (20 mL) and dichloromethane (20 mL) was refluxed for 15 h. After cooling to room temperature, and partitioned between dichloromethane and water. The water layer was extracted with dichloromethane (3×10 mL), the organic layers were combined and dried over anhydrous magnesium sulphate, filtered, purified using column chromatography (V(petroleum ether):V(ethyl acetate) = 1:1) to afford 2-[(4-methoxy-3,5-dimethyl-2-pyridinyl)methylthio]-1*H*-benzimidazole (**3a**, white solid, 99.1% purity) in 85.6% yield. m.p.: 124.0～126.6 ℃. EI-MS(m/z): 300.1(0[M+H]$^+$), 322.1([M+Na]$^+$); IR(KBr): v 3577.9, 3133.6, 3056.5, 1618.6, 1592.8, 1567.3, 1501.8, 1438.3, 1270.1, 1270.1, 1227.1, 875.1, 762.6, 734.6; ^{1}H NMR (400 MHz, Chloroform-*d*): δ 12.73 (s, 1H), 8.27 (s, 1H), 7.62 (d, J = 9.0 Hz, 1H), 7.45 (d, J = 9.0 Hz, 1H), 7.22～7.16 (m, 2H), 4.37 (s, 2H), 3.79 (s, 3H), 2.33 (s, 3H), 2.28 (s, 3H).

Similarly, 2-[(3,4-dimethoxy-2-pyridinyl)methylthio]-1*H*-benzimidazole (**3b**) was prepared as a white solid in 85.6% yield. m.p.:117.9～120.0 ℃. EI-MS(m/z): 302.1([M+H]$^+$); IR(KBr): v 3421.3, 2971.7, 2881.1, 1640.5, 1585.6, 1489.0, 1302.8, 1266.2, 1232.4, 1067.5, 820.7, 746.6. ^{1}H NMR (400 MHz, Chloroform-d): δ 13.01 (s, 1H), 8.28 (d, J = 5.6 Hz, 1H), 7.62 (s, 1H), 7.49 (s, 1H), 7.19 (dd, J = 6.0, 3.2 Hz, 2H), 6.87 (d, J = 5.6 Hz, 1H), 4.40 (s, 2H), 3.95 (s, 3H), 3.94 (s, 3H).

2-{[(3-Methyl-4-(2,2,2-trifluoroethoxyl)-2-pyridinyl)]methylthio}-1*H*-benzimidazole (**3c**) was prepared as a white solid in 88.0% yield. m.p: 149.3～150.5 ℃(lit[7]: 149～150 ℃). EI-MS(m/z): 354.1($[M+H]^+$); IR(KBr): v 3135.1, 3052.5, 2976.3, 2896.6, 2844.4, 1618.5, 1589.8, 1577.9, 1444.2, 1269.1, 1163.6, 1174.2, 1110.4, 857.9, 746.0; ^{1}H NMR (400 MHz, Chloroform-d): δ 12.57 (s, 1H), 8.43 (d, J = 5.5 Hz, 1H), 7.62 (s, 1H), 7.46 (s, 1H), 7.19 (dd, J = 6.0, 3.1 Hz, 2H), 6.74 (d, J = 5.6 Hz, 1H), 4.45 (m, 1H), 4.42 (s, 2H), 2.33 (s, 3H).

2-{[(4-(3-Methoxypropoxy)-3-methyl-2-pyridinyl]methylthio}-1*H*-benzimidazole (**3d**) was prepared as a white solid in 77.0% yield. m.p: 105.1～106.0 ℃. EI-MS(m/z): 344.1($[M+H]^+$); IR(KBr): v 3420.1, 3267.0, 3098.9, 2966.6, 2925.0, 2837.3, 1625.5, 1599.0, 1550.3, 1510.0, 1464.4, 1382.4, 1360.8, 1323.2. 1303.4, 1260.4, 1176.3, 1164.01121.3. ^{1}H-NMR (400 MHz, chloroform-d): δ 8.12 (d, J = 8.9 Hz, 2H), 7.54 (d, J = 8.6 Hz, 1H), 7.09～6.90 (m, 4H), 4.14～4.00 (m, 3H), 3.90 (s, 3H), 2.95～2.88 (m, 1H), 2.84 (dt, J = 12.5, 6.3 Hz, 1H), 2.78～2.71 (m, 1H), 2.60 (s, 3H), 1.10 (d, J = 6.3 Hz, 6H).

2. 3 Crystal structure determination

The target compound **3b** was taken a bit into a conical flask, dissolved by methanol/acetone (V/V = 1/1) mixture. The bottleneck of the flask was sealed for volatilizing slowly by plastic film. The white single crystals of the target compound **3b** (0.24mm × 0.22mm × 0.18mm) used for X-ray crystallographic analysis was obtained after 7 days. The data of **3b** were collected by a Rigaku 007HF Xta LAB P200 diffractometer equipped with a graphite-monochromatic Mo$K\alpha$ radiation (λ = 0.71073 Å) using an ω scan mode at 113 K. In the range of $3.0 \leqslant \theta \leqslant 27.5°$, a total of 18516 reflections were collected with 5388 unique ones (R_{int} = 0.0347), of which 3181 ($-11 \leqslant h \leqslant 11$, $-15 \leqslant k \leqslant 15$, $-16 \leqslant l \leqslant 17$) were observed with $I > 2\sigma(I)$ and used in the succeeding refinements. The intensity data were corrected for Lp factors and empirical absorption. The structure was resolved by direct methods and expanded by difference Fourier techniques with SHELXL and SHELXS programs[12-14]. All of the non-hydrogen atoms were located with successive difference Fourier syntheses. The structure was refined by full-matrix least-squares techniques on F^2 using anisotropic thermal parameters for all non-hydrogen atoms. The hydrogen atoms were added according to theoretical models. The final cycle of refinement converts to R = 0.0231, wR = 0.0596 ($w = 1/[\sigma^2(F_o^2) + (0.0360P)^2 + 0.1411P]$, where $P = (F_o^2 + 2F_c^2)/3$), S = 1.073, $(\Delta/\sigma)_{max}$ = 0.035, $(\Delta\rho)_{max}$ = 0.191, and $(\Delta\rho)_{min}$ = –0.168 e·Å^{-3}.

2. 4 Antitumor activity

Human liver cancer cell line HepG2 and human liver normal cell line HL7702 were used to evaluate the anti-tumor activity of target compounds *in vitro* by MTT assay with 5-fluorouracil as the positive control[15, 16]. HepG2 and HL7702 cells were harvested in the logarithmic growth phase and seeded in 96-well plates at a density of 8000 cells per well, and cultured at 37 ºC in humidified atmosphere containing 5% CO_2 in Dulbecco's modified Eagle's medium (DMEM or RPMI-1640) with 10% fetal bovine serum (FBS) for 24 h before any treatments. The tested compounds were dissolved in DMSO and diluted in the culture fluid to get various concentrations. The cells were treated with target compounds subsequently and incubated overnight. Then 20 μL of MTT (5 mg/mL) was added in each well and after 4 h incubation, the medium was removed immediately and MTT formazan was solubilized in 150 μL of DMSO. The optical densities (OD) were measured with a microplate reader (Bio-Tek instruments, INC. USA) at 490 nm. Inhibitory effects were expressed as the percentage of inhibition. Each assay was performed thrice.

3 RESULTS AND DISCUSSION

3. 1 Molecular structure

The crystal structure of the target compound **3b** (0.24 mm × 0.22 mm × 0.18 mm) was confirmed by X-ray diffraction analysis. The target compound **3b** crystallizes in orthorhombic, space group $P2_12_12_1$ with a = 9.1828(16), b = 11.625(2), c = 13.463(2) Å, V = 1437.2 (5) Å^3, Z = 4, $C_{15}H_{15}O_2N_3S$, D_c = 1.393 g cm^{-3}, μ = 0.233 mm^{-1}, F(000) = 632, S = 1.073, R = 0.0222 and wR = 0.0593 for 3181 independent reflections (Rint = 0.0347) with I > 2σ(I)). The selected bond distances and bond angles are listed in Table 1.

Table 1. Selected Bond Lengths (Å) and Bond Angles (°) for Compound 3b

Bond	Dist.	Bond	Dist.	Bond	Dist.
S(1)–C(1)	1.8091(16)	N(2)–C(9)	1.311(2)	C(5)–C(6)	1.386(3)
S(1)–C(9)	1.7489(16)	N(2)–C(15)	1.396(2)	C(10)–C(11)	1.394(2)
O(1)–C(3)	1.3740(18)	N(3)–C(2)	1.347(2)	C(10)–C(15)	1.404(2)
O(1)–C(7)	1.436(2)	N(3)–C(6)	1.337(2)	C(11)–C(12)	1.384(2)
O(2)–C(4)	1.3513(19)	C(1)–C(2)	1.512(2)	C(12)–C(13)	1.395(3)
O(2)–C(8)	1.437(2)	C(2)–C(3)	1.387(2)	C(13)–C(14)	1.385(3)
N(1)–C(9)	1.362(2)	C(3)–C(4)	1.400(2)	C(14)–C(15)	1.401(2)
N(1)–C(10)	1.385(2)	C(4)–C(5)	1.392(2)		
Angle	(°)	Angle	(°)	Angle	(°)
C(9)–S(1)–C(1)	100.84(8)	C(2)–C(3)–C(4)	119.38(14)	N(1)–C(10)–C(15)	105.28(13)
C(4)–O(2)–C(8)	117.52(13)	O(2)–C(4)–C(3)	116.11(14)	C(11)–C(10)–C(15)	122.22(15)
C(9)–N(1)–C(10)	105.87(13)	O(2)–C(4)–C(5)	125.68(15)	C(12)–C(11)–C(10)	116.91(16)
C(9)–N(2)–C(15)	103.57(13)	C(5)–C(4)–C(3)	118.21(14)	C(11)–C(12)–C(13)	121.36(16)

C(6)–N(3)–C(2)	117.09(14)	C(6)–C(5)–C(4)	117.97(15)	C(14)–C(13)–C(12)	122.02(16)
C(2)–C(1)–S(1)	114.49(11)	N(3)–C(6)–C(5)	124.65(15)	C(13)–C(14)–C(15)	117.40(17)
N(3)–C(2)–C(1)	118.78(13)	C(3)–O(1)–C(7)	113.77(12)	N(2)–C(15)–C(10)	110.32(14)
N(3)–C(2)–C(3)	122.64(14)	N(1)–C(9)–S(1)	118.55(12)	N(2)–C(15)–C(14)	129.61(16)
C(3)–C(2)–C(1)	118.58(14)	N(2)–C(9)–S(1)	126.48(12)	C(14)–C(15)–C(10)	120.07(15)
O(1)–C(3)–C(2)	120.18(13)	N(2)–C(9)–N(1)	114.97(14)		
O(1)–C(3)–C(4)	120.35(14)	N(1)–C(10)–C(11)	132.50(16)		

The molecular structures and crystal packing pictures were drawn by the Diamond program[17]. One structure unit of **3b** is shown in Fig. 1. The molecular packing for **3b** viewed along the *a* axis is depicted in Fig. 2.

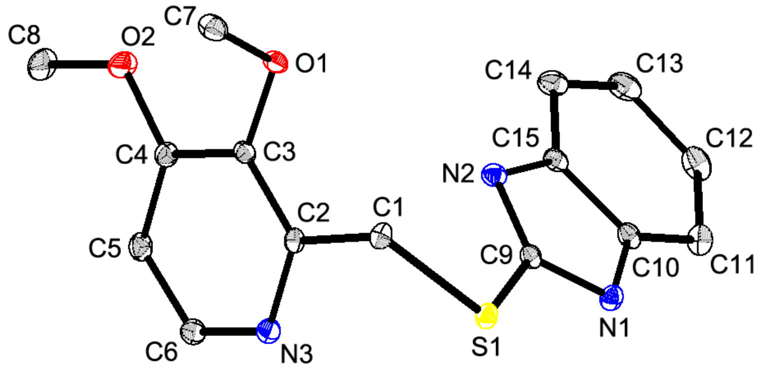

Fig. 1. Structure unit of 3b, showing the atom numbering scheme

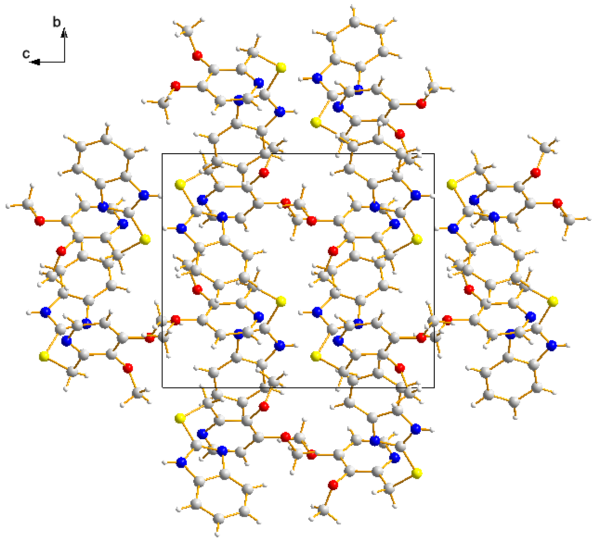

Fig. 2. Molecular packing for 3b

There are some weak interactions (donor–H···acceptor interactions, D–H···A interactions, including N–H···N, C–H···O, C–H···S, C–H···N, C–H···π interactions) observed in Fig. 3 by using the Mercury program[18], with the red dashed lines indicating the interactions. The weak interactions are listed in Table 2.

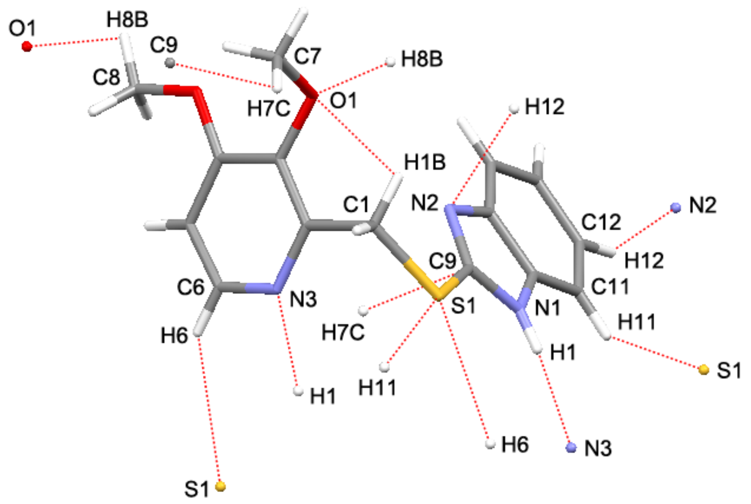

Fig. 3. Part of the crystal structure of 3b. D–H···A interactions are shown with red dashed lines

Table 2. Weak D–H···A Interactions of 3b

D–H···A	d (D–H) (Å)	d (H···A) (Å)	d (D···A) (Å)	Angle (D–H···A) (°)	Symmetry codes
N(1)–H(1)···N(3)$^{(i)}$	0.8330(215)	2.0911(216)	2.9192(20)	172.675(2066)	(i) –1/2+*x*, 1/2–*y*, 1–*z*
C(1)–H(1B)···O(1)	0.9900(16)	2.3447(11)	2.8046(20)	107.400(97)	
C(6)–H(6)···S(1)$^{(i)}$	0.9496(17)	2.8873(6)	3.6781(18)	141.471(104)	(i) –1/2+*x*, 1/2–*y*, 1–*z*
C(8)–H(8B)···O(1)$^{(ii)}$	0.9797(19)	2.4740(11)	2.8660(22)	103.528(112)	(ii) –1/2+*x*, 1/2–*y*, –*z*
C(11)–H(11)···S(1)$^{(iii)}$	0.9500(17)	2.8339(5)	3.4307(18)	121.782(105)	(iii) 1/2+*x*, 1/2–*y*, 1–*z*
C(12)–H(12)···N(2)$^{(iv)}$	0.9499(18)	2.5018(13)	3.3565(22)	149.720(112)	(iv) 1–*x*, –1/2+*y*, 1/2–*z*
C(7)–H(7C)···C(9)$^{(v)}$	0.9803(18)	2.8540(15)	3.4371(24)	118.935(109)	(v) 2–*x*, –1/2+*y*, 1/2–*z*

3. 2 Antitumor activity

Using 5-fluorouracil as a positive control, the target compounds were evaluated for the cytotoxic activities *in vitro* against human liver cancer cell line HepG2 and human liver normal cell line HL7702 by MTT colorimetric assay. The *in vitro* inhibitory activity results of the target compounds are summarized in Table 3.

Table 3. Inhibitory Activity *in vitro* of the Target Compounds

Compound	Inhibition rate (%) (50 μM)	
	HepG2	HL7702
3a	13.27	0.40
3b	28.54	1.96
3c	34.52	1.75
3d	22.29	2.21
5-Fluorouracil	100	7.33

These results show the target compounds exhibit weak or moderate cytotoxic activity against HepG2, and all the target compounds almost do not exhibit cytotoxic effects on HL7702. These results have revealed that the target compounds show excellent selective activity against the malignant tumor cell line.

4 CONCLUSION

A series of 2-[(pyridin-2-yl)methylthio]-1*H*-benzimidazole derivatives were designed, synthesized and characterized by IR, MS, and proton NMR, and the target compound 2-[(3,4-dimethoxypyridin-2-yl)methylthio]-1*H*-benzimidazole (**3b**) was investigated with X-ray crystallography. The antitumor activities of target compounds were evaluated for the cytotoxic activities against human liver cancer cell line HepG2, and human liver normal cell line HL7702 using MTT assay. The cytotoxicity assay results have showed that these target compounds exhibit weak or moderate anti-tumor activity against HepG2, while all the target compounds exhibit no cytotoxic effects on HL7702, which implies that the target compounds show excellent selective activity against the malignant tumor cell line.

ACKNOWLEDGEMENT The authors would like to thank Crystal Impact GbR Ltd. Co. and Cambridge Crystallographic Data Centre (CCDC) for kindly providing us with a free evaluation of their software packages, Diamond and Mercury. The software packages would be used strictly for individual research or teaching use. The authors thank Prof. Hai-Bin Song from Nankai University for crystal structure analysis.

REFERENCES

(1) Biemar. F.; Foti, M. Global progress against cancer — challenges and opportunities. *Cancer Biology Med*. **2013**, 10, 183-186.

(2) Spasov, A. A.; Yozhitsa, I. N.; Bugaeva, L. I.; Anisimova, V. A. Benzimidazole derivatives: spectrum of pharmacological activity and toxicological properties. *Pharm. Chem. J.* **1999**, 33, 232-243.

(3) Garuti, L.; Roberti, M.; Rossi, T.; Cermelli, C.; Portolani, M.; Malagoli, M.; Castelli, M. Synthesis, antiviral and antiproliferative activity of some N-benzenesulphonyl-2(2- or 3-pyridylethyl)benzimidazoles. *Anti-cancer Drug Des*. **1998**, 13, 397-406.

(4) Garuti, L.; Roberti, M.; De Clercq, E. Synthesis and antiviral/antiproliferative activity of some N-sulphonylbenzimidazoles. *Bioorg. Med. Chem. Lett.* **2002**, 12, 2707-2710.

(5) Buscató, E.; Büttner, D.; Brüggerhoff, A.; Klingler, F. M.; Weber, J.; Scholz, B.; Zivković, A.; Marschalek, R.; Stark, H.; Steinhilber, D.; Bode, H. B.; Proschak, E. From a multipotent stilbene to soluble epoxide hydrolase inhibitors with antiproliferative properties. *ChemMedChem*. **2013**, 8, 919-923.

(6) Yadav, S.; Narasimhan, B.; Kaur, H. Perspectives of benzimidazole derivatives as anticancer agents in the new era. *Anti-cancer Agents Med Chem.* **2015**, 16, 1403-1425.

(7) Kohl, B.; Sturm, E.; Senn-Bilfinger, J.; Simon, W. A.; Krüger, U.; Schaefer, H.; Rainer, G.; Figala, V.; Klemm, K. (H^+,K^+)-ATPase inhibiting 2-[(2-pyridylmethyl)sulfinyl]benzimidazoles. 4. A novel series of dimethoxypyridyl-substituted inhibitors with enhanced selectivity. The selection of pantoprazole as a clinical candidate. *J. Med. Chem*. **1992**, 35, 1049-1057.

(8) Liu, X. P.; Xu, H. L.; Sun, R.; Li, X.; Hu, B. H.; Hu, C. Synthesis and characterization of two impurities in esomeprazole, an antiulcerative drug.

Latin Am. J. Pharm. **2015**, 34, 1265-1268.

(9) Zhang, L.; Xu, H. L.; Deng, X. S.; Liu, C. C.; Liu, X. P.; Hu, C. Synthesis of impurity B of Esomeprazole. *Fine Chem. Intermed.* **2015**, 45, 17-19.

(10) Kaminski, J. J.; Doweyko, A. M. Antiulcer agents. 6. Analysis of the in vitro biochemical and in vivo gastric antisecretory activity of substituted imidazo[1,2-a]pyridines and related analogues using comparative molecular field analysis and hypothetical active site lattice methodologies. *J. Med. Chem.* **1997**, 40, 427–436.

(11) Terauchi, H.; Tanitame, A.; Tada, K.; Nakamura, K.; Seto, Y.; Nishikawa, Y. Nicotinamide derivatives as a new class of gastric H+/K(+)-ATPase inhibitors. 1. Synthesis and structure-activity relationships of N-substituted 2-(benzhydryl- and benzylsulfinyl)nicotinamides. *J. Med. Chem.* **1997**, 40, 313-321.

(12) Sheldrick, G. M. *SHELXL97. Program for the Refinement of Crystal Structures*. University of Göttingen: Göttingen, Germany **1997**.

(13) Sheldrick, G. M. *A short history of SHELX*. *Acta Cryst. A* **2008**, 64, 112–122.

(14) Sheldrick, G. M. Crystal structure refinement with SHELXL. *Acta Cryst. C* **2015**, 71, 3–8.

(15) Mosmann, T. Rapid colorimetric assay for cellular growth and survival: application to proliferation and cytotoxicity assays. *J. Immun. Methods* **1983**, 65, 55-63.

(16) Berridge, M. V.; Tan, A. S. Characterization of the cellular reduction of 3-(4,5-dimethylthiazol-2-yl)-2,5-diphenyltetrazolium bromide (MTT): subcellular localization, substrate dependence, and involvement of mitochondrial electron transport in MTT reduction. *Arch. Biochem. Biophys.* **1993**, 303, 474-482.

(17) Bergerhoff, G.; Berndt, M.; Brandenburg, K. Evaluation of crystallographic data with the program DIAMOND. *J. Res. Natl. Inst. Stand. Technol.* **1996**, 101, 221-225.

(18) Macrae, C.; Edgington, P.; McCabe, P.; Pidcock, E.; Shields, G.; Taylor, R.; Towler, M. J. van de Streek. Mercury: visualization and analysis of crystal structures. *J. Appl. Cryst.* **2006**, 39, 453-457.

Synthesis, Crystal Structure and Biological Activity of 2-[(Pyridin-2-yl)methylthio]-1*H*-benzimidazole Derivatives

GAO Di(高迪) CHEN Gu-Zhou(陈固洲) CAO Sheng(曹胜) DU Yue(杜月) JIN Zhe(金辄)
LIU Xiao-Ping(刘晓平) OUYANG Gui-Ping(欧阳贵平) HU Chun(胡春)

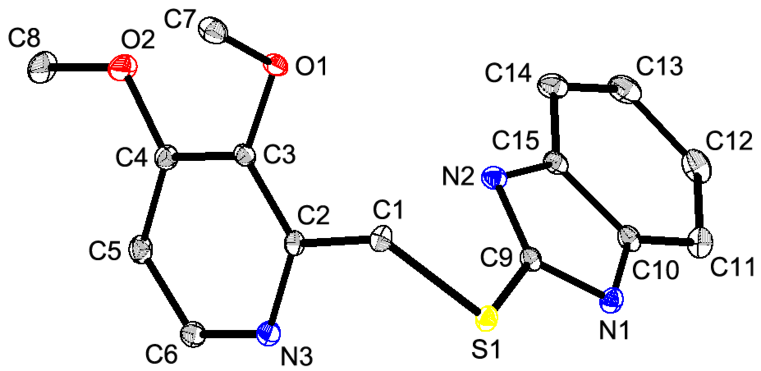

A series of 2-[(pyridin-2-yl)methylthio]-1*H*-benzimidazole derivatives were designed and synthesized, and the structures were characterized by IR, MS, and proton NMR. 2-[(3,4-Dimethoxypyridin-2-yl)methylthio]-1H-benzimidazole was investigated with X-ray crystallography.

Antitumor activities of the target compounds were evaluated against human liver cancer cell line HepG2, and human liver normal cell line HL7702 using MTT assay. The target compounds demonstrate weak or moderate anti-tumor activity against HepG2, but no cytotoxic effects on HL7702.